PCCP
Physical Chemistry Chemical Physics

Accepted Manuscript

This article can be cited before page numbers have been issued, to do this please use: M. S. Faillace, E. A. Dolgopolova, N. M. Ceballos, E. N. Ruiz Pereyra, L. Lanfri, G. A. Argüello, M. Burgos Paci, N. Shustova and W. J. Peláez, *Phys. Chem. Chem. Phys.*, 2023, DOI: 10.1039/D3CP01655B.

ROYAL SOCIETY OF CHEMISTRY

rsc.li/pccp

View Article Online
DOI: 10.1039/D3CP01655B

GFP- related Chromophores: Photoisomerization, Thermal Reversion, and DNA Labelling

Martin S. Faillace[a,b], Ekaterina A. Dolgopolova[b], Noelia M. Ceballos[a], E. Nahir Ruiz Pereyra[a], Lucia Lanfri[a], Gustavo A. Argüello[a], Maximiliano Burgos Paci[a], Natalia B. Shustova[b], Walter J. Peláez*[,a].

[a]INFIQC-CONICET-Dpto. de Fisicoquímica, Facultad de Ciencias Químicas, Universidad Nacional de Córdoba, Ciudad Universitaria, Córdoba, X5000HUA, Argentina

[b]Department of Chemistry and Biochemistry, University of South Carolina, Columbia, South Carolina 29208, United States.

Keywords

Thioxoimidazolidinones

Imidazothiazolones

Photoisomerization

Enthalpy-entropy compensation effect

Abstract

Due to pronounced effect of the confined environment on the photochemical properties of the 4-hydroxybenzylidine imidazolinone (HBI), a GFP-related chromophore, imidazolinone and imidazothiazolone analogues have been studied as fluorescent probes. Their photoisomerization and their thermal reversion were studied under 365-nm-irradiation, resulting in observance of an enthalpy-entropy compensation effect. Theoretical studies were carried out to shed light on the thermal reversion mechanism. Moreover, photophysical studies of benzylidene imidazothiazolone in the presence of dsDNA revealed fluorescence enhancement. The prepared compounds could be considered as a valuable tool for the detailed investigation of physicochemical, biochemical, or biological systems.

View Article Online
DOI: 10.1039/D3CP01655B

Introduction

Green fluorescent protein (GFP) is a broadly used imaging tool in molecular biology and in medicine to visualize various biological events.[1] The chromophore of the GFP, 4-hydroxybenzylidine imidazolinone (HBI), can isomerize from *Z* to *E* isomer. It is well known that the *Z* isomer acts as an efficient fluorophore, while the *E* configuration possesses an extremely weak fluorescence.[2] This particular behaviour is also strongly dependent on the environment that the scaffold of the protein senses, defining chromophore photophysics. For this reason, several studies with HBI analogues have been carried out and put forward the importance of the subject.[3–6]

From a different perspective, there are many studies focused on the biological activities of 5-arylmethylene imidazolidinones.[7,8] For instance, it was found that a combination of the thiocarbonyl group and C5 benzylidene substituent could be a recognition motif for P450 metabolism in a human hepatocyte model.[9] Our recent findings demonstrated the antioxidant properties as well as the modulatory activity of some imidazolidinone derivatives, along with a noteworthy light-enhanced activity against *S. aureus*.[10,11] That is, some imidazolidinone compounds were able to inhibit the growth of *S. aureus* ATCC 25923 upon UV irradiation. This last result reinforces the need for understanding the photochemical features of these heterocyclic compounds from a molecular point of view.

Moreover, fundamental understanding of the interaction of DNA with small organic molecules is crucial for the development of new drugs for cancer treatment as well as addressing overcoming bacteria resistance to antibiotics.[12,13] There are examples of this core in different applications,[14] for instance, DNA labelling,[14–16] which can be studied by emission techniques.

In our previous work, we demonstrated the experimental and theoretical evidences for photoisomerization and thermal reversion of 5-arylmethylene-2-thioxoimidazolidin-4-one.[17] Herein, we expanded the scope of considered derivatives using a number of different aryl substituents, among which there are some compounds with promising biological activities as mentioned above. Furthermore, to introduce a structural change, the sulfur atom was used to build a bicyclic moiety as shown in Scheme 1. As previously described, the environment of the HBI chromophore plays a crucial role on its photophysics,[1] encouraging us to provide deeper insights into the fluorescent properties of the heterocycles in the presence of dsDNA. Notably, these heterocycles have functional moieties for hydrogen bonding, suitable to interact with DNA. As an outcome, we believe that this work

View Article Online
DOI: 10.1039/D3CP01055B

contributes to the fundamental understanding of the photochemical properties of the HBI-related arylmethylene heterocycles.

Experimental section

Synthesis of imidazolines and imidazothiazolones (**1a-c** and **2a-c**) were performed by microwave irradiation in a monowave 300 Anton Paar, based on previously described conventional methodologies.[10,18] Imidazolines **1a-c** were purified by column chromatography ($CHCl_3$:EtOH, 90:10) while imidazothiazolones **2a-c** were purified by preparative Thin-Layer Chromatography (CH_2Cl_2:EtOAc, 80:20). All compounds were characterized using the spectroscopic techniques including NMR (1D- & 2D) and UV-vis spectroscopy as well as mass spectrometry; all acquired data are in agreement with the proposed structures.

UV-vis spectra of chromophores in acetonitrile (HPLC grade) were recorded on a UV-1601 Shimadzu spectrophotometer using a quartz cell with an optical path length of 1-cm.

The reaction yields for the compounds **2a-c** were determined by HPLC. Elution was performed with a mixture of CH_3OH:H_2O (90:10) at a flow rate of 0.8 mL min^{-1}. The experiments were performed employing a Waters 1525 Binary Pump connected to a Waters 2998 Photodiode Array Detector, and a C18 column (5 µm × 4.5 µm × 15 cm).

For characterization of the compounds, NMR spectra were recorded in DMSO-d_6 and acetone-d_6 on a Bruker Avance II 400 MHz spectrometer (BBI probe, z gradient) (^{1}H at 400.16 MHz, ^{13}C at 100.56 MHz and ^{19}F at 376.53 MHz) at 22 °C. Chemical shifts are reported in parts per million (ppm) downfield from TMS.

Gas chromatography/mass spectrometry (GC/MS) analyses were performed on Shimadzu GC-MS-QP 5050 spectrometer equipped with a VF column (30 m × 0.25 mm × 5 µm) using helium as eluent at a flow rate of 1.1 mL min^{-1}. The injector and ion source temperature were 280 °C, the pressure in the MS instrument was 10^{-5} Torr, and MS recordings were made in the electron impact mode (EI) at ionization energy of 70 eV.

The photoisomerization and the thermal reversion were monitored by the integration of the ^{1}H NMR spectra between 45–75 °C. For this purpose, a Bruker Avance III-HD 300 MHz spectrometer was used. A 365-nm LED lamp (M365L2, Thorlabs) was used as an excitation source. The corresponding solutions were prepared in CD_3CN.

To investigate the electronic structure and potential energy surfaces of (**1a-c** and **2a-c**), we have used *ab initio* quantum chemistry. No symmetry constraints were imposed neither on molecular geometries nor electronic wave functions. Optimization and vibrational frequencies of the ground state geometries were performed at the B3LYP/6-311+g(d,p) level. To confirm the transition state structures, frequency and intrinsic reaction coordinate (IRC) calculations were performed.

The complete active space–self-consistent field (CASSCF) method was used to obtain the excited electronic state (T_1). This method is described by the number of states included in the average (*N*) and the number of electrons (*n*) and orbitals (*m*) included in the active space. The five orbitals that constitute the active space are the HOMO-2, HOMO-1, HOMO, LUMO, and LUMO+1, as previously described.[17] All stationary potential energy points, including electronic state minima and degeneracies, were optimized with SA-2-CAS(6/5) method. The 6-31G(d) basis set was used for all CASSCF calculations.

The time-dependent density functional theory (TD-DFT/6-311+g(d,p) was used to model the energies and properties of the electronically excited states. We have included solvent contributions using the PCM solvent model at S_0 and T_1. All calculations were performed with Gaussian 09.[19]

The fluorescent profile was examined in the absence and presence of fish dsDNA (0.029 %P/P). DNA solutions were prepared in TE buffer (Tris 10 mM, EDTA 1mM, pH 7.5). The sample solutions were initially diluted in DMSO, rising a final concentration of 0.3 mM in the cuvette (16 %V/V DMSO). A solution of ethidium bromide (EtBr) at 15 μM was used as a positive control. All the analyses were performed at a controlled temperature (30 °C). Fluorescence spectra were measured using a PTI QM2 (Quanta Master 2) spectrofluorometer from Photon Technology International which utilizes a pulsed Xe lamp (75 W) as the excitation source and a photon-counting detector. An excitation wavelength of 307 nm was used, and the fluorescence spectra were recorded in the range from 350 to 750 nm.

Results and Discussion

Synthesis

A series of the HBI-related analogues were prepared using a microwave synthesis as described in Scheme 2. As described in our previous work, 5-arylmethylene thioxoimidazolidinones (**1a-c**) were prepared through the condensation reaction of thiohydantoin with different aromatic aldehydes (path A), in 69–96 % yields.[10] The 5-arylmethylene imidazothiazolone derivatives were prepared using

two different synthetic approaches. First approach for the synthesis of imidazothiazolones (**2a-c**) was based on the reaction of (**1a-c**) with 1,2-dichloroethane. However, this synthetic route had some limitations due to hydrolysis of the desired product. Efforts to improve the synthetic procedure (see ESI for more details) led to the second approach which includes the one-pot synthesis described in Scheme 2 (path B), that turned out to be the efficient procedure to prepare benzylidene imidazothiazolone derivatives (e.g., compound **2a**, 98 % yield).

The formation of **2a** could be postulated considering two different pathways. It is known that thiohydantoin is in equilibrium with the thiol tautomer;[20,21] for this reason, the nucleophilic attack to the alkyl group could be initiated either by the thiol group or the nitrogen lone pair of the thiohydantoin. To address this question, a reaction of 1-bromoethane with **1a** was performed. As shown in Scheme 3, if the reaction occurred via the nitrogen, compound **3** should be detected, while compound **4** would be identified if the nucleophilic attack occurred via the sulphur atom. After completion of the reaction, compound **4** resulted as the main product of the reaction. Additionally, a sub-product that incorporated two ethyl groups was also detected (**5**). These compounds were elucidated by ^{1}H-NMR spectroscopy and GC/MS, as shown in Figures S1 and S2 in the ESI.

Photoisomerization and thermal reversion

Our heterocyclic compounds (**1a-c** and **2a-c**) were almost exclusively in the *Z* form. In addition, they presented similar strong absorption bands between 340 and 380 nm, as shown in section 4 of ESI. In the previous publication, we demonstrated that photoisomerization of **1a** is a monophotonic process occurring through the rotation of the dihedral angle (τ) in a biradical pathway.[17] In this work, we explored photochemical behaviour of other derivatives, with different substituents on the phenyl group: one electron-donating group by inductive effect (**1b**) and an electron-withdrawing substituent (**1c**). Moreover, compounds **2a-c** were designed with the purpose of re-functionalize the heterocyclic moiety, leading to the more planar structures, which favours their interaction with DNA.[16]

Solutions of arylidene heterocycles were prepared in CD_3CN due to the high viscosity of DMSO-d_6, which drastically increased their thermal reversion times. The isomerization and thermal reversion (Scheme 1) was monitored by ^{1}H NMR spectroscopy following the signal of the vinyl hydrogen. The concentration of each isomer was calculated by integration of ^{1}H NMR spectra at different irradiation times. The samples were isomerized using a 365-LED lamp leading to the increase of the *E* isomer concentration with time until a photostationary state (PSS) is achieved as shown in Figure 1.

At 25 °C, only compounds **1a** and **1c** have measurable concentration of the *E* isomer, since the methylated derivative **1b** and all the bicyclic compounds (**2a-c**) have the *Z* conformation exclusively. Regarding the compound **1b**, its conformation can be attributed to the size of the methyl substituent and its solvent box, which precludes isomerization at room temperature. Moreover, our findings are in line with the observations for 5-arylmethylenehydantoins studied by of Tan *et al*.[22], who suggested that the *Z/E* equilibrium ratio is higher with the electron-donating groups on the benzene ring.[22]

Interestingly, compounds **1a-c** reach the PSS, with a higher concentration of the Z isomer. In contrast to the fused imidazothiazolidinone (**2a-c**), for which the concentration of the *E* isomer predominates (Table 1).

Once the PSS was achieved, and after stopping the irradiation, the *E*-isomers were thermally isomerized to the *Z* conformation in a unimolecular process.[17] This process was very slow and despite our attempts to advance isomerization with acetic acid, either in DMSO-d_6 or CD_3CN, no net effect was observed. Moreover, the samples after reaching the PSS were irradiated at 590 nm to induce the photo-reversion reaction as it was previously reported by Tan *et al* on 5-arylmethylenehydantoin;[23] but after 50 min of irradiation, no changes in the concentration of either isomers were detected.

Thermal *E*→Z isomerization of compounds **1a-c** and **2a-c** (Scheme 3) was investigated as a function of temperature (from 45 to 75 °C) in CD_3CN. As an instance of thermal reversion progress is shown for the compound **2a** at 45 and 75 °C (Figure 2). The complete set of exponential decays is detailed in the Supporting Information. The Arrhenius plots for the studied compounds are shown in Figure 3. The use of the Eyring equation gave a complete determination of the activation parameters which are detailed in Table 2. The equations used to determine physicochemical parameters are presented in the Supporting Information (page S17).

The process "photoisomerization-thermal reversion" was repeated for several cycles without apparent decomposition of the studied compounds, meaning that both isomers are thermally (45–75 °C) as well as photochemically (under 365-nm irradiation) stable.

The evaluated isomerization rate constant (*k*) of the bicyclic compounds (**2a-c**) is 1.3 to 3-fold higher than that calculated for thioxoimidazolidinones **1a-c**. Previous reports for GFP-chromophore analogues mention that an electron-withdrawing group at the phenyl moiety accelerates the thermal isomerization when the addition/elimination mechanism takes place.[24,25] However, in our findings, the isomerization rates of the compounds with a fluorine substituent (**1c** and **2c**) are lower than those

View Article Online
DOI: 10.1039/D3CP01655B

of the other derivatives. This result is congruent with our previous result where the mechanism operating is through a diradical pathway.[17]

At the same time, the Van't Hoff plot in Figure 4 denotes the lack of an intersection point, which emphasizes that there is not an isokinetic effect, as it can be expected due to the differences in the isomerization rates shown in Table 2. For this reason, it is challenging to evaluate thermodynamic enthalpy of these processes. Nevertheless, as it is indicated in Table 2, free energies of activation are very similar, and consequently, a compensation effect was observed in the enthalpy-entropy correlation plot, as shown in Figure 4. The correlation coefficient of the linear plot (0.9998) can be used as a criterion for this assumption.[26]

Theoretical calculations

As previously proposed for compound **1a**, thermal isomerization from *E* to *Z* species would be accomplished through the formation of a biradical intermediate via an S_0–T_1 intersystem crossing (ISC) which is less energetic than simple twisting.[17] In this work, we performed further calculations in both the gas phase and solution, where the polarizable conductor calculation model of solvation (CPCM) was used to extend our assumption to the whole set of compounds.

Ground state B3LYP/6-311+g(d,p) gas-phase calculations show that *Z* isomers of **1a-c** and **2a-c** are more stable than their *E* counterparts by approximately 2–4 kcal mol^{-1}. Moreover, the gas-phase barrier for $E \rightarrow Z$ conversion through simple dihedral rotation is about 63–75 kcal mol^{-1} and 48–71 kcal mol^{-1} **1a-c** and **2a-c**, respectively (Table 3).

To achieve a better fit of the theoretical values with the experimental ones, we have performed CPCM calculations (in acetonitrile as a solvent) implemented in Gaussian. This particular solvent was chosen because thermal reactions, monitored by the NMR spectroscopy, were also performed in acetonitrile-d_3. In this case, the calculated values of the energy barrier for the isomerization *E* - *Z* are lower in energy than those obtained in the gas phase. For instance, for the compounds **1a-c** the energy barriers in acetonitrile are almost 10 kcal mol^{-1} lower in comparison with the gas phase values while for the cycled compounds (**2a-c**) are almost 5 kcal mol^{-1} more stable in solution than in gas phase (Table 3). In all cases, a twisted conformation corresponds to the transition state, which is characterized by its zwitterionic nature. Therefore, the potential energy surfaces in solution (PESs, S_0 and T_1) were calculated for all compounds studied herein. These calculations are weight evidence on the reaction pathway proposed in our previous article for **1a**,[17] via a biradical species (Scheme **4**, paths **a,b,c**), which is lower in energy compared to the simple twisting of the double bond of the benzylidene moiety

for all the compounds (Scheme **4**, paths **d,e**). This finding allows us to extrapolate the mechanism proposed for **1a** to other studied compounds, even for derivatives obtained through changing the functionality of the sulphur atom in the bicyclic counterparts.

As can be seen in Figure 5 for **2a-c** and Figure S6 for the rest, the T_1 surface presents lower energy than the maximum of S_0, still having a minimum at almost 100° which is very similar to the one obtained for the maximum of S_0. In addition, when analysing the PES for the ground state (S_0) and T_1 along the *E*→Z torsional pathway, two ISCs (ISC-I and ISC-II) were found. The energy values of these two points are very similar, being slightly more energetic for the simpler derivatives (**1a-c**), as shown in Table 3. The fact that the biradical channel over single torsion in the ground state is the most plausible, suggesting that thermal isomerization could occur via a triplet state, achieved by an ISC between the S_0 and T_1 surfaces, for all the compounds under study, as it was demonstrated before for compound **1a**.[17] All other relevant parameters can be found in the ESI.

On the other hand, we calculated the theoretical activation entropy ($\Delta S^{\#}$), activation enthalpy ($\Delta H^{\#}$), and activation free energy ($\Delta G^{\#}$) required for thermal reversion (E→Z) via the S0-T1(ISC-II)-S0 pathway (Table 3). Based on these studies, it was found a good correlation between the calculated and experimental $\Delta G^{\#}$ at the same temperature. As expected, at temperatures lower than the boiling point of the solvent (acetonitrile-d_3, b.p.: 80 °C) render the energy for the thermal reversion.

It is noteworthy, that within each family, the larger the cross-section coefficient (logε), the greater the percentage of the *E* isomer in the PSS (Table 2). Additionally, the ISC-II energies of compound **2a-c** are lower compared to the corresponding values for **1a-c**, which correlate with the higher proportion of the less stable isomer *E*. Therefore, the proportion of isomers in the PSS is given by a combination of the effects produced by these parameters on photoisomerization and thermal reversion. which could raise an explanation for the change in the isomers ratio of both compounds upon irradiation.

In our previous work, fully unconstrained optimizations were recalculated at the CASSCF level (CAS(6/5)/6-31g(d)) of the PES (S_0 and T_1) of **1a** in order to shed light on thermal reversion. Nevertheless, the method failed due to the intrinsic lack of the correction for the correlation energy. In the present work, we calculated all barriers for a new set of thioxoimidazolidinone (**1b-c**) and imidazothiazolone **(2a-c)** derivatives with the same method and basis set used for **1a**.[17] Here again, the obtained energy barrier was overcoming, in accordance with the experimental results, thus, we conclude that energy correction is crucial in these kinds of calculations.

View Article Online
DOI: 10.1039/D3CP01655B

DNA interaction

In order to evaluate if there is an interaction between dsDNA and some of our derivatives (namely **1a** and **2a**, which were selected as representative models), their luminescence properties were studied. These compounds are good candidates as fluorescent probes due to their planar structure and the heteroatoms that may form hydrogen bonds. It was already studied that there is a DNA interaction with some 5-benzylidene-hydantoin[27] and 5-benzylidene-thiohydantoin;[16] however, to the best of our knowledge, there are no studies in the literature with the imidazothiazolones presented in this work.

As it was explained above, the photoisomerization of these compounds is well established. This process is the main cause of their low emission in solution. However, an enhancement of the emission should be observed if the fluorophore is trapped in a confined environment.[28] Nevertheless, due to the isomerization E→Z is a thermal controlled process, the reason why all the experiments about dsDNA interactions were performed at 30°C is due through NMR it was observed that in solution only Z isomer is present at temperatures above 30°C for all compounds.

The fluorescent profile was examined in the absence and presence of fish dsDNA (0.025 %P/P in buffer TE). Solutions of the samples (**1a** and **2a**) were prepared in DMSO reaching a final concentration of 300 μM. Ethidium bromide (EtBr) was employed as positive control and it was used at a lower concentration of 15 μM due to its self-quenching.

The results are shown in Figure 6, where the emission of the compounds is compared with and without the presence of dsDNA (after 4 hours of incubation at 30 °C). It can be observed that compound **2a** interacts better with dsDNA than the other molecules. When dsDNA is added to a solution of **2a** the fluorescence increased up to eightfold. In addition, the emission maxima present a blueshift from 452 nm (free molecule) to 437 nm (molecule-DNA complex). This interaction, though not completely disentangled, could be understood by assuming that **2a** retains its planar structure after non-specific binding with DNA, while this could not be the case for **1a**. Nevertheless, both chromophores are compounds that possesses benzylidene-imidazolidin-one moiety which could suggest that both have a similar mode of interaction with dsDNA involving a π-π stacking interaction between the aromatic arylmethylene moiety and the base pairs of dsDNA or through the heteroatoms that may form hydrogen bonds. It seems to be generally accepted that the enhanced fluorescence is consistent with the strength of intercalative interaction. In this case, the results are indicating that compound **2a** binds more strongly than **1a**, penetrating more deeply into, and stacking more strongly

with base pairs of dsDNA. This can be rationalized since **2a** has a larger planar area and more extended π system than **1a**, acquiring a higher rigidity in its interaction within the grooves of dsDNA. The difference in planarity can be observed from the calculated dihedral angles for the styryl moiety for **1a** and **2a**, which are 21.29° and 0.09° respectively (figure S7, page S17 in the Supporting Information). In turn, due compound **1a** would bind more weakly to the dsDNA, it would have a greater conformational freedom allowing the existence of rotamers, which creates additional conformational disorder to that generated by its own prototropic tautomerism.

Regardless of the higher concentration of studied compounds in contrast to EtBr, we believe that compound **2a** could perform as a fluorescent probe because its emission appears well within the visible region besides of its reduced toxicity. Additionally, its interaction with DNA can lead to a candidature for further trial as anticancer drugs.

Conclusion

In this contribution, the synthesis and photoisomerization studies of a family of 5-arylmethylene thioxoimidazolidinone and imidazothiazolones are presented. Kinetics parameters were determined experimentally, and the results denote an enthalpy-entropy compensation effect for the series of reactions under study. Although a major part of molecular switches is based on azobenzenes, the GFP-like chromophores presented in this work could be considered in the design of molecular photoswitches due to their thermal and photochemical stability.

The preliminary investigations about the labelling of dsDNA with thioxoimidazothiazolone **2a** are promising. Further investigations are needed to understand the interaction mechanism and fluorescence effects, as well as with different molecular scaffolds.

Acknowledgements

The authors are grateful for support from the NSF Award (DMR-2103722) and SC EPSCoR GEAR. The work at the Instituto de Investigaciones en Fisicoquímica de Córdoba (INFIQC) was supported by Consejo Nacional de Investigaciones Científicas y Técnicas (CONICET grant number: PIP 11220170100423CO), Fondo para la Investigación Científica y Tecnológica (FONCyT grant number: PICT-2017-1555) and Secretaría de Ciencia y Tecnología (SeCyT -UNC grant number: SeCyT-Nº411/18). MSF thanks for the fellowship from Fulbright and CONICET. This work used

View Article Online
DOI: 10.1039/D3CP01055B

computational resources from *CCAD-UNC* (http://ccad.unc.edu.ar/), in particular the Mendieta Cluster, which is part of SNCAD-MinCyT.

Conflicts of interest

There are no conflicts to declare

Author contribution statement

MSF: investigation, validation, formal analysis (DFT calculations), writing – first draft. EAD: investigation, validation. NMC: investigation, formal analysis (DFT calculations). ENRP: investigation, formal analysis (DFT calculations). LL: investigation, validation. GAA: reviewing and editing. MBP: writing – first draft. NBS: conceptualization, formal analysis, reviewing, and editing. WJP: Conceived and designed the experiments, conceptualization, formal analysis, writing – reviewing, and editing.

References

[1] M. Zimmer, Green Fluorescent Protein (GFP): Applications, Structure, and Related Photophysical Behavior, Chem. Rev. 102 (2002) 759–782. https://doi.org/10.1021/cr010142r.

[2] H. Niwa, S. Inouye, T. Hirano, T. Matsuno, S. Kojima, M. Kubota, M. Ohashi, F.I. Tsuji, Chemical nature of the light emitter of the Aequorea green fluorescent protein, PNAS. 93 (1996) 13617–13622. https://doi.org/10.1073/pnas.93.24.13617.

[3] H. Deng, C. Yu, D. Yan, X. Zhu, Dual-Self-Restricted GFP Chromophore Analogues with Significantly Enhanced Emission, J. Phys. Chem. B. 124 (2020) 871–880. https://doi.org/10.1021/acs.jpcb.9b11329.

[4] M. Ikejiri, H. Kojima, Y. Fugono, A. Fujisaka, Y. Chihara, K. Miyashita, Synthesis and properties of geometrical 4-diarylmethylene analogs of the green fluorescent protein chromophore, Org. Biomol. Chem. 16 (2018) 2397–2401. https://doi.org/10.1039/C8OB00208H.

[5] A. Singh, S. Karmakar, I.M. Abraham, D. Rambabu, D. Dave, R. Manjithaya, T.K. Maji, Unraveling the Effect on Luminescent Properties by Postsynthetic Covalent and Noncovalent Grafting of GFP Chromophore Analogues in Nanoscale MOF-808, Inorg. Chem. 59 (2020) 8251–8258. https://doi.org/10.1021/acs.inorgchem.0c00625.

[6] E.A. Dolgopolova, T.M. Moore, O.A. Ejegbavwo, P.J. Pellechia, M.D. Smith, N.B. Shustova, A metal-organic framework as a flask: photophysics of confined chromophores with a benzylidene imidazolinone core, Chem. Commun. 53 (2017) 7361–7364. https://doi.org/10.1039/C7CC02253K.

[7] R. Saito, M. Hoshi, A. Kato, C. Ishikawa, T. Komatsu, Green fluorescent protein chromophore derivatives as a new class of aldose reductase inhibitors, European Journal of Medicinal Chemistry. 125 (2017) 965–974. https://doi.org/10.1016/j.ejmech.2016.10.016.

[8] M.-Y. Wang, Y.-Y. Jin, H.-Y. Wei, L.-S. Zhang, S.-X. Sun, X.-B. Chen, W.-L. Dong, W.-R. Xu, X.-C. Cheng, R.-L. Wang, Synthesis, biological evaluation and 3D-QSAR studies of imidazolidine-2,4-dione derivatives as novel protein tyrosine phosphatase 1B inhibitors, European Journal of Medicinal Chemistry. 103 (2015) 91–104. https://doi.org/10.1016/j.ejmech.2015.08.037.

[9] S.Q. Tang, Y.Y.I. Lee, D.S. Packiaraj, H.K. Ho, C.L.L. Chai, Systematic Evaluation of the Metabolism and Toxicity of Thiazolidinone and Imidazolidinone Heterocycles, Chem. Res. Toxicol. 28 (2015) 2019–2033. https://doi.org/10.1021/acs.chemrestox.5b00247.

[10] M.S. Faillace, A.P. Silva, A.L.A.B. Leal, L.M. da Costa, H.M. Barreto, W.J. Peláez, Sulfurated and oxygenated imidazoline derivatives: synthesis, antioxidant activity and light-mediated antibacterial activity, ChemMedChem. n/a (n.d.). https://doi.org/10.1002/cmdc.202000048.

[11] M.S. Faillace, A.L. Alves Borges Leal, F. Araújo de Oliveira Alcântara, J.H.L. Ferreira, J.P. de Siqueira-Júnior, C.E. Sampaio Nogueira, H.M. Barreto, W.J. Peláez, Inhibition of the NorA efflux pump of S. aureus by (Z)-5-(4-Fluorobenzylidene)-Imidazolidines, Bioorganic & Medicinal Chemistry Letters. 31 (2021) 127670. https://doi.org/10.1016/j.bmcl.2020.127670.

[12] P.D. Halley, C.R. Lucas, E.M. McWilliams, M.J. Webber, R.A. Patton, C. Kural, D.M. Lucas, J.C. Byrd, C.E. Castro, Daunorubicin-Loaded DNA Origami Nanostructures Circumvent Drug-Resistance Mechanisms in a Leukemia Model, Small. 12 (2016) 308–320. https://doi.org/10.1002/smll.201502118.

[13] F. Yang, S.S. Teves, C.J. Kemp, S. Henikoff, Doxorubicin, DNA torsion, and chromatin dynamics, Biochimica et Biophysica Acta (BBA) - Reviews on Cancer. 1845 (2014) 84–89. https://doi.org/10.1016/j.bbcan.2013.12.002.

[14] J. Riedl, P. Ménová, R. Pohl, P. Orság, M. Fojta, M. Hocek, GFP-like Fluorophores as DNA Labels for Studying DNA–Protein Interactions, J. Org. Chem. 77 (2012) 8287–8293. https://doi.org/10.1021/jo301684b.

[15] M. Ikejiri, M. Tsuchino, Y. Chihara, T. Yamaguchi, T. Imanishi, S. Obika, K. Miyashita, Design and Concise Synthesis of a Novel Type of Green Fluorescent Protein Chromophore Analogue, Org. Lett. 14 (2012) 4406–4409. https://doi.org/10.1021/ol301901e.

[16] A.G. Majouga, A.V. Udina, E.K. Beloglazkina, D.A. Skvortsov, M.I. Zvereva, O.A. Dontsova, N.V. Zyk, N.S. Zefirov, Novel DNA fluorescence probes based on 2-thioxo-tetrahydro-4H-imidazol-4-ones: synthetic and biological studies, Tetrahedron Letters. 53 (2012) 51–53. https://doi.org/10.1016/j.tetlet.2011.10.118.

[17] A.J. Pepino, M.A. Burgos Paci, W.J. Peláez, G.A. Argüello, An experimental and theoretical study of the photoisomerization and thermal reversion on 5-arylmethylene-2-thioxoimidazolidin-4-one, Phys. Chem. Chem. Phys. 17 (2015) 12927–12934. https://doi.org/10.1039/C4CP04748F.

[18] A.J. Pepino, W.J. Peláez, M.S. Faillace, N.M. Ceballos, E.L. Moyano, G.A. Argüello, (S)-5-Benzyl- and 5-benzylidene-imidazo-4-one derivatives synthesized and studied for an understanding of their thermal reactivity, RSC Adv. 4 (2014) 60092–60101. https://doi.org/10.1039/C4RA11046C.

[19] M.J. Frisch, G.W. Trucks, H.B. Schlegel, G.E. Scuseria, M.A. Robb, J.R. Cheeseman, G. Scalmani, V. Barone, B. Mennucci, G.A. Petersson, Gaussian 09, revision E. 01 Inc, Wallingford CT. (2009).

[20] E.G. Jayasree, S. Sreedevi, A DFT study on protic solvent assisted tautomerization of heterocyclic thiocarbonyls, Chemical Physics. 530 (2020) 110650. https://doi.org/10.1016/j.chemphys.2019.110650.

[21] S. Bagheri, H. Roohi, Proton-Transfer Mechanism in 2-Thioxoimidazolidin-4-one: A Competition between Keto/Enol and Thione/Thiol Tautomerism Reactions, BCSJ. 82 (2009) 446–452. https://doi.org/10.1246/bcsj.82.446.

[22] S.-F. Tan, K.-P. Ang, G.-F. How, Thermal equilibration of Z- and E-isomers of 5-arylmethylenehydantoins. Evidence for non-bonded aromatic π⋯ methyl attractions, J. Chem. Soc., Perkin Trans. 2. (1988) 2045–2049. https://doi.org/10.1039/P29880002045.

[23] S.-F. Tan, K.-P. Ang, G.-F. How, Z/E, photoisomerization of 5-arylmethylenehydantoins and 5-pyridylmethylenehydantoins, J. Phys. Org. Chem. 4 (1991) 707–713. https://doi.org/10.1002/poc.610041202.

[24] J. Dong, F. Abulwerdi, A. Baldridge, J. Kowalik, K.M. Solntsev, L.M. Tolbert, Isomerization in Fluorescent Protein Chromophores Involves Addition/Elimination, J. Am. Chem. Soc. 130 (2008) 14096–14098. https://doi.org/10.1021/ja803416h.

[25] J.-J. Xu, R. Sung, K. Sung, S1/S0 Potential Energy Surfaces Experience Different Types of Restricted Rotation: Restricted Z/E Photoisomerization and E/Z Thermoisomerization by an Out-of-Plane Benzyl Group or In-Plane m-Pyridinium Group?, J. Phys. Chem. A. 123 (2019) 4708–4716. https://doi.org/10.1021/acs.jpca.9b02924.

[26] L. Liu, Q.-X. Guo, Isokinetic Relationship, Isoequilibrium Relationship, and Enthalpy−Entropy Compensation, Chem. Rev. 101 (2001) 673–696. https://doi.org/10.1021/cr990416z.

[27] A. Shah, E. Nosheen, S. Munir, A. Badshah, R. Qureshi, Z.- Rehman, N. Muhammad, H. Hussain, Characterization and DNA binding studies of unexplored imidazolidines by electronic absorption spectroscopy and cyclic voltammetry, Journal of Photochemistry and Photobiology B: Biology. 120 (2013) 90–97. https://doi.org/10.1016/j.jphotobiol.2012.12.015.

[28] A. Fürstenberg, M.D. Julliard, T.G. Deligeorgiev, N.I. Gadjev, A.A. Vasilev, E. Vauthey, Ultrafast Excited-State Dynamics of DNA Fluorescent Intercalators: New Insight into the Fluorescence Enhancement Mechanism, J. Am. Chem. Soc. 128 (2006) 7661–7669. https://doi.org/10.1021/ja0609001.

View Article Online
DOI: 10.1039/D3CP01655B

SCHEMES

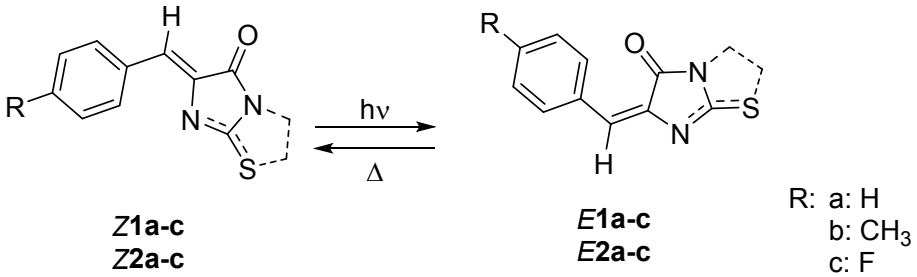

Scheme 1. Photoisomerization *Z*→*E* and thermal reversion *E*→*Z*.

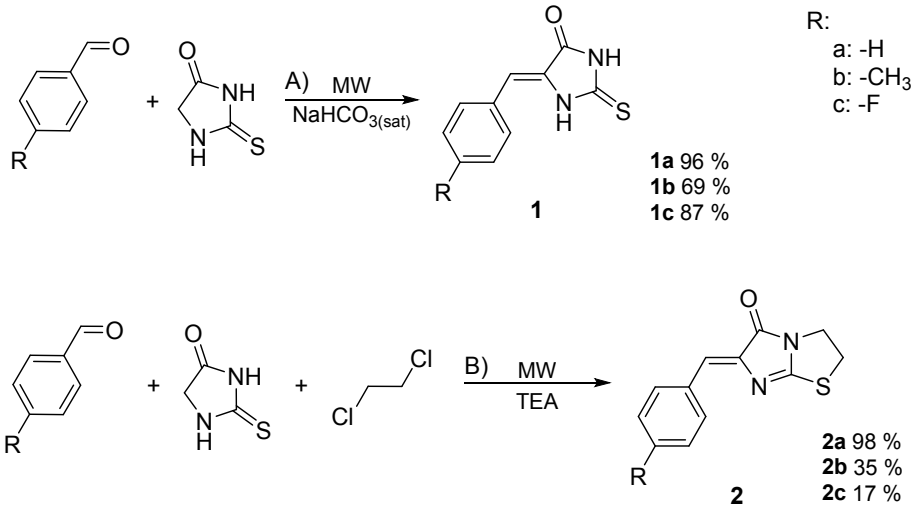

Scheme 2. Synthesis of arylidene thioxoimidazolidinones (**1a-c**) and imidazothiazolones **(2a-c)** derivatives.

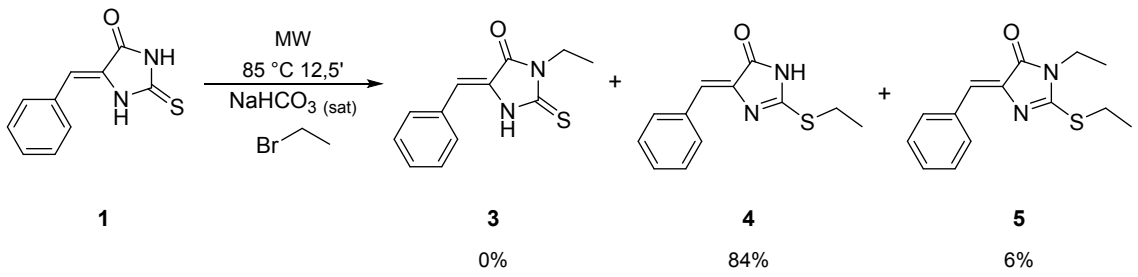

Scheme 3. Experimental mechanistic study in the formation of **2a**.

View Article Online
DOI: 10.1039/D3CP01655B

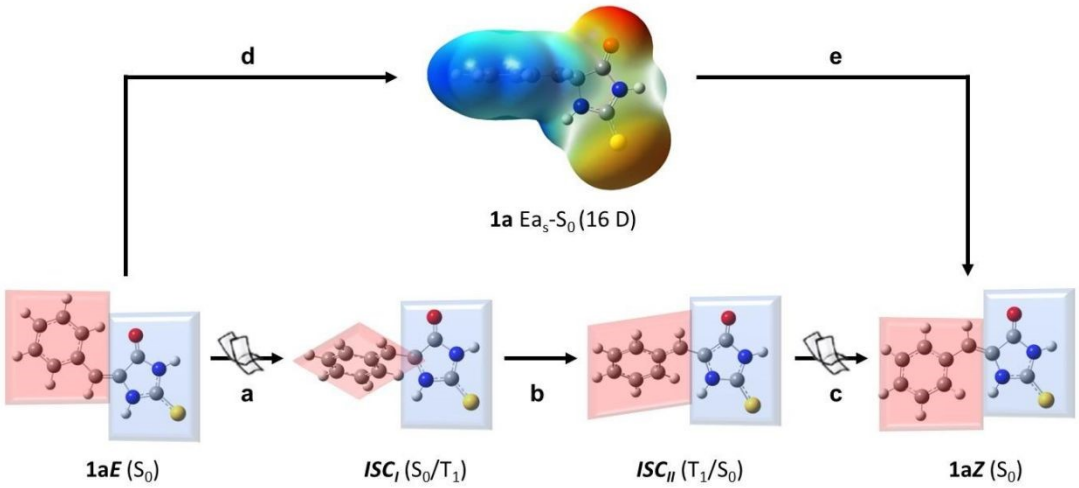

Scheme 4. Proposed isomerization reaction pathways: paths **a-b-c** through biradical species and paths **d-e** through a simple twist of the double bond.

FIGURES

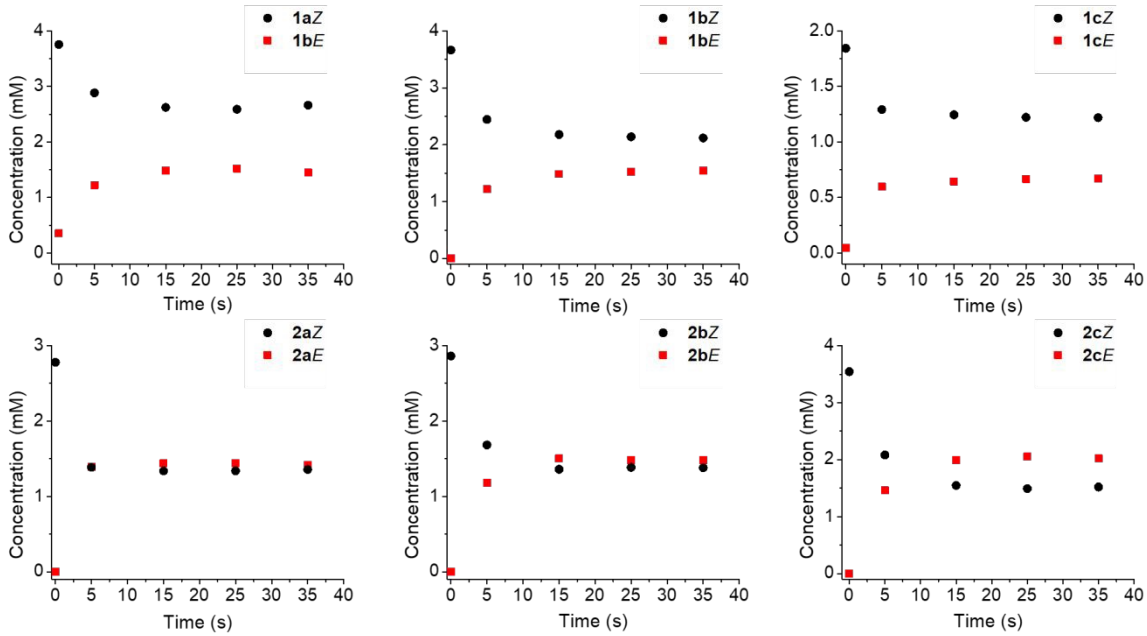

Figure 1. Formation of *E* isomer and *Z* consumption until achieving the photostationary state of the thioxoimidazolidinones and imidazothiazolones compounds **1a-c** and **2a-c**.

View Article Online
DOI: 10.1039/D3CP01655B

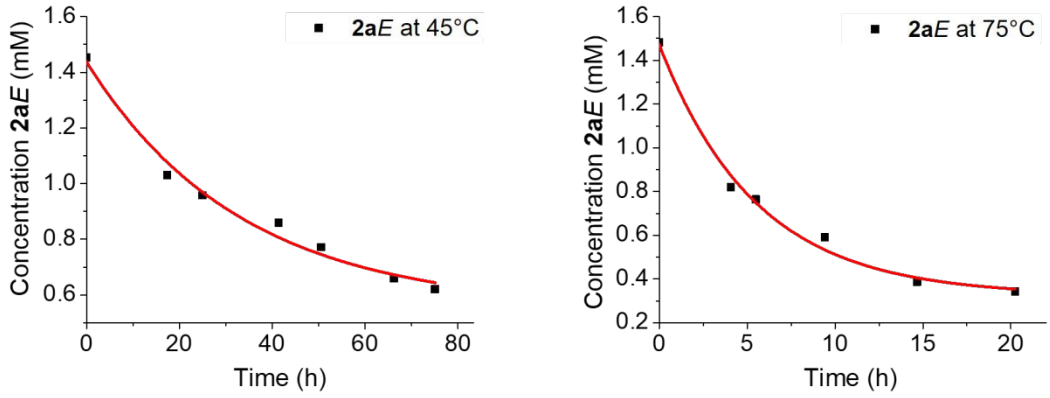

Figure 2. Temporary exponential decay of the **2a***E* isomer at two temperatures, (left) 45 and (right) 75 °C.

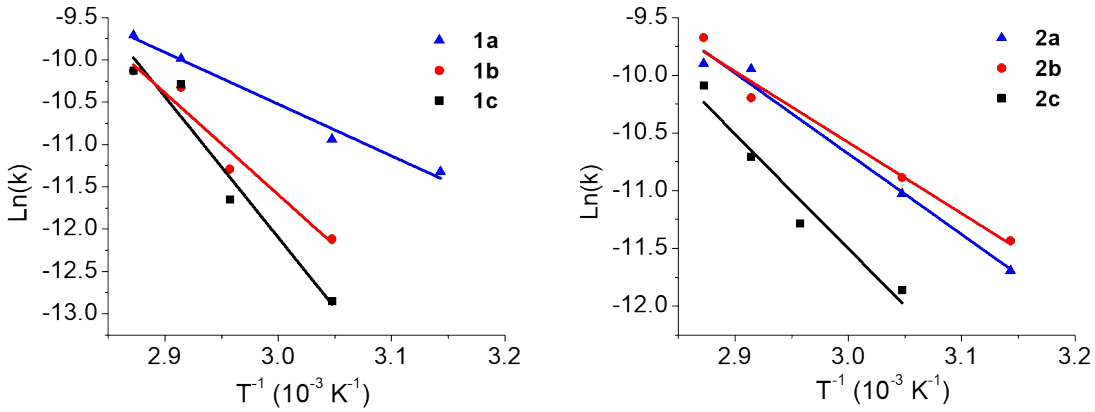

Figure 3. Arrhenius plot for all analyzed compounds.

View Article Online
DOI: 10.1039/D3CP01655B

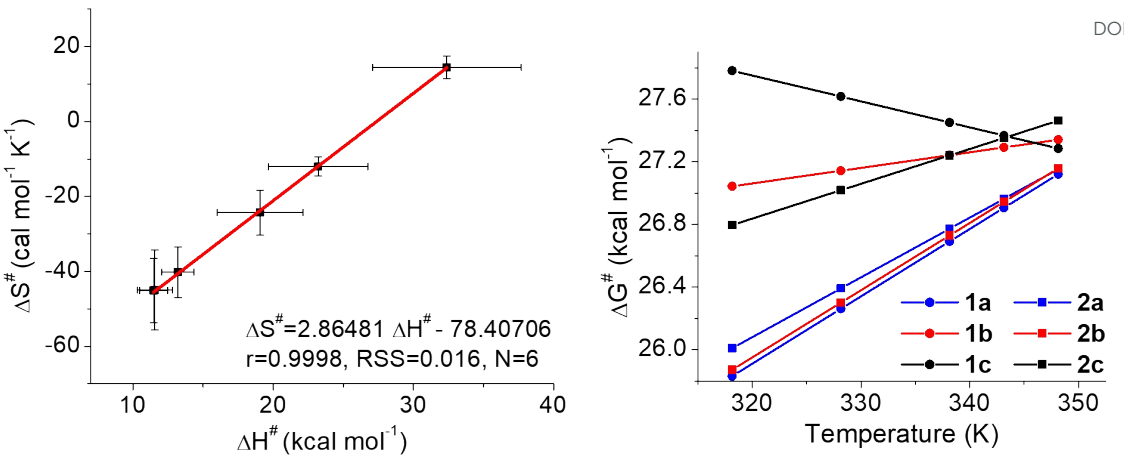

Figure 4. Enthalpy-entropy compensation plot (left) and Van't Hoff plot (right).

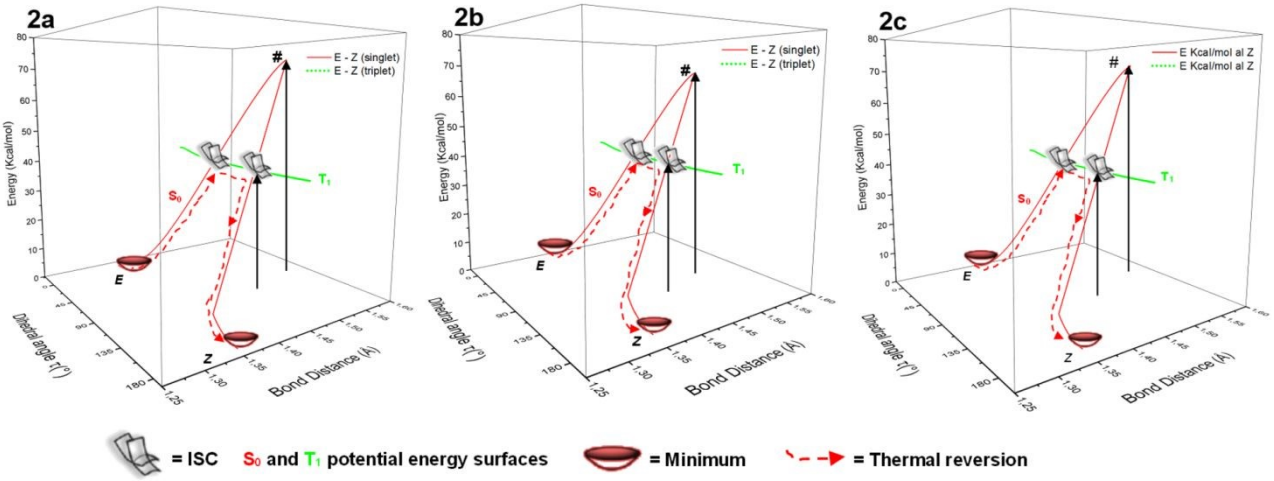

Figure 5. S_0 and T_1 potential energy surfaces (PES) obtained for compounds **2a-c**.

View Article Online
DOI: 10.1039/D3CP01655B

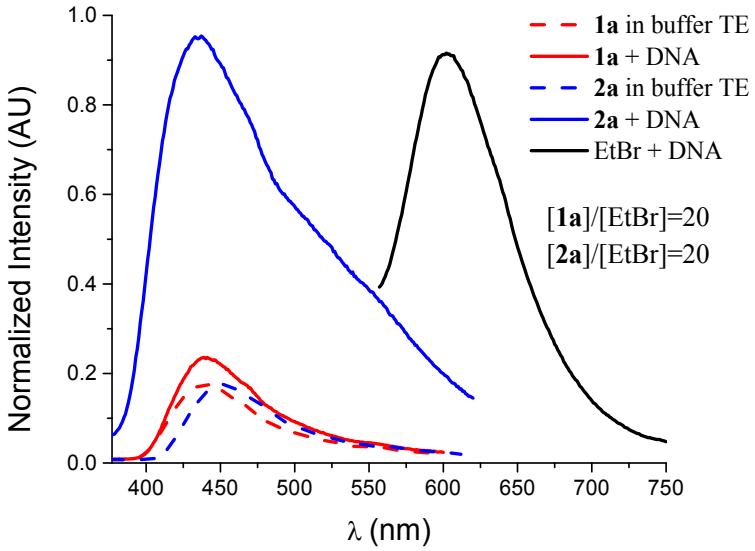

Figure 6. dsDNA interaction with the thioxoimidazolidinone and imidazothiazolone compounds.

TABLES

Table 1. Thermal equilibrium and photostationary state population of *Z/E* isomers.

Compounds	Thermal equilibrium	Photostationary state	log (ε)
	Z:E (%)	*Z:E* (%)	
1a	91:9	65:35	4.25
1b	100:0	58:42	4.55
1c	98:2	65:35	4.49
2a	100:0	49:51	4.31
2b	100:0	48:52	4.45
2c	100:0	43:57	4.97

View Article Online
DOI: 10.1039/D3CP01655B

Table 2. Kinetic and activation parameters for $E \rightarrow Z$ thermal isomerization.

Compounds	k (10^{-5} s^{-1})	log(A)	$\Delta S^{\#}$ (cal K^{-1} mol^{-1})	Ea (kcal mol^{-1})	$\Delta H^{\#}$ [a] (kcal mol^{-1})	$\Delta G^{\#}$ [a] (kcal mol^{-1})
1a	1.3	3.4	-45.0	12.2	11.5	26.9
1b	1.3	10.6	-11.9	23.9	23.2	27.3
1c	0.9	16.4	14.6	33.1	32.4	27.4
2a	1.7	4.5	-40.1	13.9	13.2	27.0
2b	3.7	3.4	-44.9	12.2	11.6	26.9
2c	1.3	7.9	-24.2	19.7	19.1	27.4

[a] calculated at 65 °C.

Table 3. Energetic and thermodynamic parameters calculated by using Gaussian09 (B3LYP/6-311+g(d,p))[a,b]

Compound	Gas phase (S_0)		Acetonitrile solution (S_0)		Acetonitrile solution (T_1)			Parameters calculated to ISC_{II}		
	Z	Ea_g-S_0	Z	Ea_s-S_0	T_1 min	ISC_I	ISC_{II}	$\Delta S^{\#}$	$\Delta H^{\#}$	$\Delta G^{\#,c}$
1a	-2,5	75.2	-2.3	62.0	36.6	36.8	38.2	4.0	36.9	35.7
1b	-2,4	63.5	-2.2	55.9	36.6	36.7	37.8	3.4	37.1	35.4
1c	-1,9	75.4	-1.9	64.0	36.9	37.0	38.5	3.8	37.3	36.1
2a	-3,4	48.5	-3.7	48.5	36.0	36.0	36.1	5.9	34.6	32.8
2b	-3,3	53.3	-3.6	49.1	36.1	36.1	36.1	4.9	34.6	33.1
2c	-3,4	70.7	-3.7	66.2	36.2	36.3	36.3	5.8	34.8	33.1

[a] Energy values are reported in Kcalmol^{-1}, except for $\Delta S^{\#}$ which is reported in cal K mol^{-1} (ue).
[b] Values reported in contrast to the E isomer. [c] Values calculated at 65 °C.